Josephson junction scheme for observing the non-Abelian statistical properties of Majorana fermions

Meng-Qing Yu,[1] Zhen-Gang Zhu,[1,2,3,*] and Gang Su[4,†]

[1]*School of Physical Sciences, University of Chinese Academy of Sciences, Beijing 100049, China*

[2]*School of Electronic, Electrical and Communication Engineering, University of Chinese Academy of Sciences, Beijing 100049, China*

[3]*CAS Center for Excellence in Topological Quantum Computation, University of Chinese Academy of Sciences, Beijing 100049, China*

[4]*Kavli Institute for Theoretical Sciences, University of Chinese Academy of Sciences, Beijing 100190, China*

(Received 8 December 2022; accepted 9 March 2023; published 27 March 2023)

Since Majorana zero mode (MZM) was proposed applicable for topological quantum computing, the past two decades have witnessed a growth of theoretical and experimental advances. Here we propose a Josephson junction setup consisting of intrinsic topological superconductors, and show that with the exchange operation of two MZMs, the single-electron tunneling current will reverse sign as a result of its non-Abelian statistics, which can be further utilized to read out the initial qubit of the system. This work offers a way to demonstrate the non-Abelian statistical properties of MZMs.

DOI: 10.1103/PhysRevB.107.094518

I. INTRODUCTION

Majorana fermions, first introduced as a solution of Dirac equations which satisfies the symmetric form of electrons and positrons by Majorana in the 1930s [1], remain as one of the central questions in modern physics. Unlike electrons and positrons, the antiparticles of Majorana fermions are exactly themselves. It has not been confirmed in particle physics since this exotic particle was predicted, while it is speculated that neutrinos might be this kind of fermions, and more works in future experiments are needed. In superconducting systems, the intrinsic particle-hole symmetry facilitates the emergence of Majorana fermions, and based on this, multiple theoretical proposals [2–6] and experimental candidates have been made in a large amount of works [7–18].

The reason that such states are of great interest stems from their intrinsically nonlocal nature and exotic exchange properties as one of the most promising approaches to realize topological quantum computing. The fermionic state which encodes the quantum information formed by two Majorana zero modes (MZMs) can develop into a highly delocalized one, and accordingly it can immune most types of decoherence. The exchange property is originated from their non-Abelian statistics, first proposed in two-dimensional (2D) systems by Read and Green [19], implying that a pairwise exchange operation in two dimensions can distinguish the initial and final state by a unitary-matrix instead of a scalar phase factor. The exchange of anyons can be described by the interlacing of their world lines in a space-time diagram, so-called "braiding," the operation that can implement quantum gates, leading to Majorana fermions that could be promising candidates to perform fault-tolerant quantum evolutions, which is one of the essential issues in topological quantum computation [20–22]. To show the existence of MZMs, most of the experiments are based on the observation of one local MZM through tunneling experiments [23–25] or zero bias conductance peak [8,26–28]. Whereas, the direct evidence that can verify MZMs is their non-Abelian statistics, which means the adiabatic operations, such as the slowly adiabatic exchange of quasiparticle positions, can bring the system from one ground state to another, instead of acquiring a phase factor in Abelian cases. However, it still remains elusive to find a measurable physical quantity to clearly characterize it under exchange operations, which limits the potential of MZMs in future application of quantum computation.

We propose a setup to show this remarkable non-Abelian property of Majorana fermions in intrinsic topological superconductors that can be relatively easy to implement in experiment. A crucial evidence of MZMs is the zero bias conductance peak (ZBCP) that has been observed in the vortex core on the surface of $FeTe_xSe_{1-x}$ [14,28,29]. Although some other non-Majorana factors such as Kondo effect, coherent Andreev reflection, and disorder-induced zero-energy states may also induce a ZBCP, they can be excluded and the MZMs are most possibly identified in experiments [10,30–32], manifesting a highly simplified single-material platform to realize MZMs. Most importantly, since each MZM is bound to the cores of vortices, this enables us to manipulate the MZMs via moving the vortices, and the manipulation of an individual vortex can be manipulated by heat [33], magnetic force [34,35], or strain-induced scanning local probe microscopies [36]. In iron-based superconductors, to avoid intermediate quasiparticle poisoning during the coherent transport of the vortex, the allowed timescales for this kind of braiding operation range from adiabatically slowup to nanoseconds, where more details will be given below.

*zgzhu@ucas.ac.cn
†gsu@ucas.ac.cn

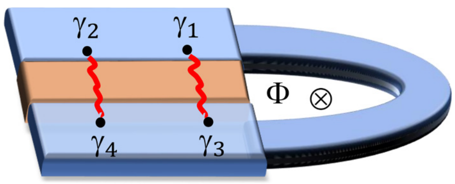

FIG. 1. A schematic setup of a superconductor-insulator-superconductor (SIS) Josephson junction. Each intrinsic topological superconductor contains MZMs at the location of Abrikosov vortices on its surface, four of which are indicated by $\gamma_1, \gamma_2, \gamma_3, \gamma_4$. γ_1 and γ_2 are close enough to couple with each other, and so are γ_3 and γ_4. The two superconducting films are connected with the same superconducting wires away from the junction, completing an S-I-S circuit with supercurrent. A flux Φ by a solenoid is penetrated through the semiring.

II. TESTING THE NON-ABELIAN STATISTICS THROUGH JOSEPHSON CURRENT

Fractional Josephson effect was first predicted by Kitaev [37], who proved that the MZMs can carry the Josephson current with a 4π-periodic current-phase relation $I \propto \pm \sin \frac{\phi}{2}$, half of the conventional Josephson junction, where ϕ is the Josephson phase and the plus/minus sign represents the fermionic parity defined by the two MZMs. The fractional ac Josephson effect in a hybrid semiconductor-superconductor InSb/Nb nanowire junction was taken as strong evidence of the existence of MZMs [7]. The sign of the current can be used to detect the fermion parity which encodes the qubit information. However, the braiding operation in a one-dimensional (1D) system is still difficult to implement in experiment. Instead, we propose a SQUID-like Josephson junction setup for this purpose as shown in Fig. 1.

The system consists of two topological superconductor films, which are deposited on the surface of an insulator forming a superconductor-insulator-superconductor (SIS) junction, and in the presence of an out-of-plane magnetic field, we presume that there are four MZMs in four spatially well-separated Abrikosov vortex cores. Two of them on each side of the superconductor can hybridize to each other through the insulator forming a single-electron state, which allows the tunneling of the single electron through the junction. The two superconducting films are connected via a half-ring forming a “hole” between the SIS and the ring, made by the same superconductor, threading a flux Φ by a solenoid through the hole (see Fig. 1), which can be used to tune the phase difference $\phi = \phi_1 - \phi_2$ between the two superconductors. Since we have the Bogoliubov–de Gennes (BdG) Hamiltonian of $FeTe_{0.55}Se_{0.45}$ [38], then similar to Eq. (B1), the Hamiltonian of this Josephson junction can be written as

$$\mathcal{H}_{\mathrm{BdG}} = \begin{pmatrix} -\frac{\hbar^2\left(k_x^2+k_y^2\right)}{2m} - \mu + U_0\delta(x) & \frac{\Delta_\beta}{p_{\mathrm{F}}}(p_x + ip_y) \\ \frac{\Delta_\beta}{p_{\mathrm{F}}}(p_x - ip_y) & \frac{\hbar^2\left(k_x^2+k_y^2\right)}{2m} + \mu - U_0\delta(x) \end{pmatrix}, \tag{1}$$

where U_0 represents a barrier potential at the interface between the upper and lower superconductors, and β refers to the upper or lower one, $\Delta_{\mathrm{U}} = \Delta_0 e^{i\phi_1}$ and $\Delta_{\mathrm{L}} = \Delta_0 e^{i\phi_2}$, with Δ_0 the bulk gap of the superconductor. It is theoretically expected that the $s_\pm$ bulk superconductivity of $FeTe_{0.55}Se_{0.45}$ single crystals endows Dirac surface states with s-wave superconducting pairing through the proximity effect in k space [39], leading to effective spinless $p_x + ip_y$ superconductivity on the surface [40]. As a result, the normal Josephson current in our system reads (i.e., the Cooper-pair current)

$$I_{\mathrm{N}} = I_{\mathrm{s}} + I_{\mathrm{p}}. \tag{2}$$

Here we take the pairing symmetry of the bulk state as s wave approximately for convenience, and according to Appendix B, the normal Josephson current I_{sx} and I_{px} can be obtained in the 1D Josephson junction SIS based on s-wave superconductors and p-wave superconductors separately:

$$I_{sx} = \frac{e\Delta_0 D \sin\phi}{\hbar\sqrt{1 - D\sin^2\frac{\phi}{2}}},$$
$$I_{px} = \frac{e\Delta_0}{\hbar}\sqrt{D}\sin(\phi/2), \tag{3}$$

where $D = \frac{4}{Z_0^2+4}$ is the transmission coefficient of the barrier in Josephson junction with $Z_0 = \frac{2mU_0}{\hbar^2 k_{\mathrm{F}}}$. We select the coordinate axis x perpendicular to the Josephson junction plane, by assuming that the interface between the two superconductors is smooth enough, the electron momentum components k_y and k_z, parallel to the junction plane, is a conserved good quantum number. Then the 2D or 3D problem separates into a set of 1D solutions in the x direction labeled by the indices k_y and k_z. As for the $p_x + ip_y$ wave in our system, the Fermi momentum k_{F} is replaced by their x components $k_x = \sqrt{k_{\mathrm{F}}^2 - k_y^2}$; therefore the transmission coefficient D of the barrier becomes k_y dependent:

$$D(k_y) = \frac{4}{Z^2(k_y) + 4}, \tag{4}$$

with $Z(k_y) = Z_0\frac{k_F}{\sqrt{k_F^2 - k_y^2}}$. Consider that the number of propagating channels of the $x-y$ plane is $N_y = Wk_{\mathrm{F}}/\pi$ [41], where W_y is the length in the y direction of the Josephoson junction. So under the zero temperature approximation, we have $-k_{\mathrm{F}} \leqslant k_y \leqslant k_{\mathrm{F}}$, which means the corresponding k_y in the nth channel can be written as $k_{ny} = -k_{\mathrm{F}} + \frac{2\pi n}{W_y}$. Therefore the Josephson current in the junction based on the $p_x + ip_y$ superconductors should be written as a function of k_{ny}, which reads

$$I_{\mathrm{p}} = \sum_{n=0}^{N_y} I_{px}(k_{ny}). \tag{5}$$

The same procedure may be easily adapted to obtain I_{s} in a three-dimensional isotropic s-wave superconductor in our system:

$$I_{\mathrm{s}} = \sum_{n=0}^{N_y}\sum_{m=0}^{N_z} I_{sx}(k_{ny}, k_{mz}), \tag{6}$$

with $N_z = \frac{W_z k_F}{\pi} N_y$ and $k_{mz} = -k_F + \frac{2\pi m}{W_z}$, where W_z is the length in the z direction of the Josephoson junction.

Now the fractional Josephson current induced by the MZM tunneling should be taken into account too. Among the four MZMs, γ_1 and γ_2 (γ_3 and γ_4) pair up to form a fermionic state with energy E_{12} (E_{34}) and occupancy $\hat{n}_{12}$ ($\hat{n}_{34}$) which are defined as

$$\begin{aligned}\hat{n}_{12} &= \hat{d}_1^\dagger \hat{d}_1,\\ \hat{n}_{34} &= \hat{d}_2^\dagger \hat{d}_2,\end{aligned} \tag{7}$$

where $\hat{d}_1$ is the annihilation operator of the fermionic state with the transformation

$$\begin{aligned}\hat{d}_1 &= \tfrac{1}{2}(\gamma_1 + i\gamma_2),\\ \hat{d}_2 &= \tfrac{1}{2}(\gamma_3 + i\gamma_4).\end{aligned} \tag{8}$$

Combining the fact that the superconducting order parameter is the product of the wave function of two electrons, and a MZM is the linear superposition of an electron and a hole, the phase of a MZM is half of the superconducting phase, which means from Eq. (8) we can obtain $\gamma_1 \propto (\hat{d}_1 e^{i\phi_1/2} + \hat{d}_1^\dagger e^{-i\phi_1/2})$, $\gamma_2 \propto \frac{1}{i}(\hat{d}_1 e^{i\phi_2/2} - \hat{d}_1^\dagger e^{-i\phi_2/2})$. Therefore the coupling Hamiltonian of γ_1 and γ_2 can be given by $H_{\Gamma_{12}} \propto i\gamma_1\gamma_2 = i(\hat{d}_1 e^{i\phi_1/2} + \hat{d}_1^\dagger e^{-i\phi_1/2})\frac{1}{i}(\hat{d}_1 e^{i\phi_2/2} - \hat{d}_1^\dagger e^{-i\phi_2/2}) = \cos\frac{\phi}{2}(2\hat{d}_1^\dagger \hat{d}_1 - 1)$. As a result, considering the effect of superconducting phase difference, the coupling Hamiltonian of all four MZMs in our system can be written as

$$H_\Gamma = \cos\left(\frac{\phi}{2}\right)(i\Gamma_1\gamma_1\gamma_2 + i\Gamma_2\gamma_3\gamma_4), \tag{9}$$

where Γ_1 and Γ_2 are the corresponding coupling strengths. Substituting Eq. (8) into it, we have

$$H_\Gamma = \cos\left(\frac{\phi}{2}\right)[\Gamma_1(2\hat{d}_1^\dagger \hat{d}_1 - 1) + \Gamma_2(2\hat{d}_2^\dagger \hat{d}_2 - 1)]. \tag{10}$$

It is supposed that the four MZMs are spatially well separated, which means $E_{12}, E_{34} \approx 0$. And the conservation of parity is also assumed, i.e., the occupation of ground state can only be even or odd, and cannot change from one to another under adiabatic operations. Without loss of generality, the initial parity of our system is presumed to be even (for the odd parity case, the calculation is similar and the results remain unchanged); therefore, there are two fermionic states stemming from the four MZMs. By combining the two fermionic states together, we have two degenerate ground states: $|0_{12}0_{34}\rangle$ and $|1_{12}1_{34}\rangle$. For simplicity we will omit the subscripts in the following discussion. Then the state of these four MZMs should be a superposition of the above ground states as $|\psi\rangle = \alpha|00\rangle + \beta|11\rangle$, which means, every time we conduct a current measurement, the state will collapse into $|00\rangle$ or $|11\rangle$, leading to the single-electron current (i.e., the fractional Josephson current induced by the MZM tunneling [37])

$$I_{\mathrm{MZM}} = \frac{2e}{\hbar}\frac{d\langle H_\Gamma\rangle}{d\phi} = \pm\frac{2e}{\hbar}(\Gamma_1 + \Gamma_2)\sin\frac{\phi}{2} \propto \sin\frac{\phi}{2}, \tag{11}$$

where $\langle H_\Gamma\rangle$ is the expectation value for $\langle 00|H_\Gamma|00\rangle$ or $\langle 11|H_\Gamma|11\rangle$. Obviously the current exhibits a 4π periodicity with ϕ, and $\pm$ depends on the system states ($|00\rangle$ or $|11\rangle$). The derived 4π periodicity is similar to that in the 1D Josephson system [42]. Although theoretically we can read out the qubit by measuring the direction of I_{MZM}, there may be still some difficulties in experiments, such as to separate I_{MZM} from I_{N} [consisting of I_{s} and I_{p}; see Eq. (2)] and extra dc current signal. Hence to distinguish them more intuitively in experiment, we consider one more step that brings γ_1 around γ_3 and back to its original position in the end. In other words, we first measure the current with keeping the MZMs immobile, and then measure the current again after circulating γ_1 around γ_3. After the first measurement, we suppose the state of this system collapses into $|00\rangle$. According to the definition of the exchange operator of MZMs [20], $B_{13} = \sqrt{\frac{i}{2}}(1 + \gamma_1\gamma_3)$, and from Eq. (8) we know that γ_1 and γ_3 can be written as $\hat{d}_1 + \hat{d}_1^\dagger$ and $\hat{d}_2 + \hat{d}_2^\dagger$, thus we have

$$\begin{aligned}|00\rangle \to B_{13}^2|00\rangle &= i\gamma_1\gamma_3|00\rangle\\ &= i(\hat{d}_1 + \hat{d}_1^\dagger)(\hat{d}_2 + \hat{d}_2^\dagger)|00\rangle = i|11\rangle,\end{aligned} \tag{12}$$

which means, after this circling operation (exchange them twice), the state $|00\rangle$ is tuned into state $|11\rangle$, so that the direction of the fractional Josephson current through this Majorana channel will be reversed according to Eq. (11), implying that we can detect an increase of total current measurement, which uniquely stems from their non-Abelian statistics. As for the other circumstance, i.e.. $|11\rangle$ is taken as the initial state, then the braiding operation will lead our system to a $|00\rangle$ state, resulting in a decrease in total current.

III. ESTIMATION OF THE SIZE AND TRANSMISSION COEFFICIENT OF THE JOSEPHSON JUNCTION

As we have discussed above, the difference of the fractional Josephson current after the braiding operation is the very observable quantity that can verify the non-Abelian statistics of MZMs in our system. Now due to the fact that the total current $I = I_{\mathrm{MZM}} + I_{\mathrm{N}}$ is the physical quantity we can measure in experiments, and the Cooper-pair tunneling will not be affected by the braiding operation of MZMs, we can detect the change of state $|00\rangle \to |11\rangle$, through the difference of total current between the first current measurement and the second after the braiding operation (for simplicity we set $\Gamma_1 = \Gamma_2 = \Gamma$):

$$\begin{aligned}\Delta I &= \frac{4e}{\hbar}(\Gamma_1 + \Gamma_2)\sin\frac{\phi}{2} - \left[-\frac{4e}{\hbar}(\Gamma_1 + \Gamma_2)\sin\frac{\phi}{2}\right]\\ &= \frac{8e}{\hbar}\Gamma\sin\frac{\phi}{2} = 2I_{\mathrm{MZM}}.\end{aligned} \tag{13}$$

Furthermore, to clearly distinguish the difference of I_{MZM} between two total-current measurements, the relative magnitudes of these two are qualitatively calculated in the following. When the distance between two vortices is much larger than the superconducting coherence length $R \gg \xi$, the wave function of MZM located at one vortex core is exponentially small at the core region of the other vortex [see in Eq. (A17)]. In this case, the vortices can be regarded as independent. When they are closer, but still remain a weak-coupling state, the effect of coupling between the MZMs must be taken into account, leading to an energy splitting of the original degenerate ground states $|00\rangle$ and $|11\rangle$. The splitting energy in $FeTe_{0.55}Se_{0.45}$ may be exploited by [38,43]

$$\Gamma \approx -\frac{2\Delta_{\text{surface}}}{\pi^{3/2}}\frac{\cos\left(k_F R + \frac{\pi}{4}\right)}{\sqrt{k_F R}}\exp\left(-\frac{R}{\xi}\right), \tag{14}$$

where ξ is the superconducting coherent length, k_F is the Fermi momentum of the surface Dirac cone in a general $p_x + ip_y$ superconductor system, and Δ_{surface} is the superconducting gap of the surface state. As for the Dirac surface state of $FeTe_{0.55}Se_{0.45}$, we have $\Delta_{\text{surface}} = 1.8$ meV, $k_F = 0.2\ \text{nm}^{-1}$, $\xi = v_F/\Delta_{\text{surface}} = 13.9$ nm [40,44]. Then as we have discussed above, we can reasonably assume that the ratio of ΔI and I should satisfy

$$r = \frac{\Delta I}{I} = \frac{\Delta I}{I_{\text{MZM}} + I_p + I_s} \geqslant 0.1 \tag{15}$$

to make ΔI large enough compared with I to become observable in experiments, which produces the relation [combining Eqs. (11) and (13)]

$$I_p + I_s \leqslant 19 I_{\text{MZM}}. \tag{16}$$

Here we assume $R = 90\ \text{nm} = 6.47\xi$, and with Eq. (A17), we can obtain $|\Psi(r)|^2 \propto 10^{-6}$, i.e., the wave function of this MZM is approximately small enough at the core region of the other, suggesting that the precondition for the establishment of Eq. (14) is fulfilled, and thus the magnitude of I_{MZM} can be evaluated with Eqs. (14) and (11). As for I_p and I_s, involving the summation of all currents with all possible k_y, so as to simplify the evaluation, the maximum currents $I_p^{\max}$ and $I_s^{\max}$ are taken into account. Obviously once the relation

$$I_s^{\max} + I_p^{\max} \leqslant 19 I_{\text{MZM}} \tag{17}$$

is fulfilled, Eq. (16) will automatically hold. Based on this fact, with Eqs. (3) and (4), we can find that, with the minimum momentum $|k_y|^{\min}$, i.e., $k_y = 0$, I_{px} will take the maximum value as $I_{px}^{\max} = I_{px}(k_y = 0) = \frac{e\Delta_0}{\hbar}\sqrt{D}\sin\frac{\phi}{2}$. Further considering the relation in Eq. (5), we can obtain the maximum of I_p approximately with

$$I_p^{\max} < N_y I_{px}^{\max} = \frac{W_y k_F e\Delta_0}{\pi\hbar}\sqrt{D}\sin\frac{\phi}{2}. \tag{18}$$

As for I_s, with the limitation $D \ll 1$ in Eq. (3):

$$I_{sx} \approx \frac{e}{\hbar}\Delta_0 D\sin\phi, \tag{19}$$

and similarly we have

$$I_s^{\max} < N_y N_z I_{sx}^{\max} = \frac{2W_y W_z k_F^2 e\Delta_0}{\pi^2\hbar} D\sin\phi. \tag{20}$$

Now we substitute the results of Eqs. (18) and (20) into Eq. (17), leading to

$$\frac{W_y k_F e\Delta_0}{\pi\hbar}\sqrt{D}\sin\frac{\phi}{2} + \frac{2W_y W_z k_F^2 e\Delta_0}{\pi^2\hbar} D\sin\phi \leqslant 19 I_{\text{MZM}}, \tag{21}$$

where the superconducting gap of the bulk state of $FeTe_{0.55}Se_{0.45}$, $\Delta_0 \approx 3$ meV [40], thus we can obtain an estimation as follows:

$$1.88 W_y\sqrt{D} + 0.24 W_y W_z D \leqslant 0.17, \tag{22}$$

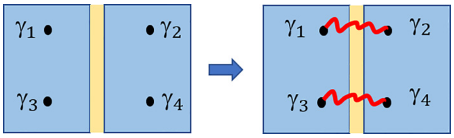

FIG. 2. A schematic of a Majorana qubit that hosts four spatially separate MZMs. γ_1 and γ_2, and γ_3 and γ_4 are paired separately. The red wavy lines indicate the coupling between them.

which is the very relation that should be satisfied to ensure that the change of the Majorana-induced fractional Josephson current ΔI between two measurements can be observable in experiment. In addition, in the limit of $W_z \to 0$, we have

$$W_y\sqrt{D} \leqslant 0.09\ \text{nm}. \tag{23}$$

For example, if the width of the y direction of the juntion $W_y \sim 1\ \mu$m, as a result, the transmission coefficient of the barrier should be $D \leqslant 9.5 \times 10^{-3}$ at most.

IV. READING OUT A QUBIT AND TESTING NON-ABELIAN FUSION RULES

Furthermore, we study the way of reading out an arbitrary qubit through projective measurements based on this setup as shown in Fig. 2. Four MZMs are spatially well separated in the beginning, hence the initial state is $|\psi_i\rangle = \alpha|00\rangle + \beta|11\rangle$. Next γ_1 and γ_2, and γ_3 and γ_4 are put close to make them weakly coupled as a consequence of the wave-function overlapping to lift the double degeneracy between the two states of $|00\rangle$ and $|11\rangle$. Finally a Josephson current measurement is implemented; then we restore the system to its original state and repeat the above steps several times, and hence there will be a probability of $|\alpha|^2$ to obtain I_{MZM} as $\frac{4e}{\hbar}\Gamma\sin\frac{\phi}{2}$ or $|\beta|^2$ as $-\frac{4e}{\hbar}\Gamma\sin\frac{\phi}{2}$, indicating that we can read out the basic state ($|00\rangle$ or $|11\rangle$) of the initial qubit through the magnitude of the total Josephson current:

$$I = \begin{cases} I_N - \frac{4e}{\hbar}\Gamma\sin\frac{\phi}{2} \to |00\rangle(|\alpha|^2) \\ I_N + \frac{4e}{\hbar}\Gamma\sin\frac{\phi}{2} \to |11\rangle(|\beta|^2), \end{cases} \tag{24}$$

In view of the above results, the proposal of testing the non-Abelian fusion can also be achieved as shown in Fig. 3. Four MZMs are coupled to each other initially and different ways of separation will lead to different final states [45]. For the upper

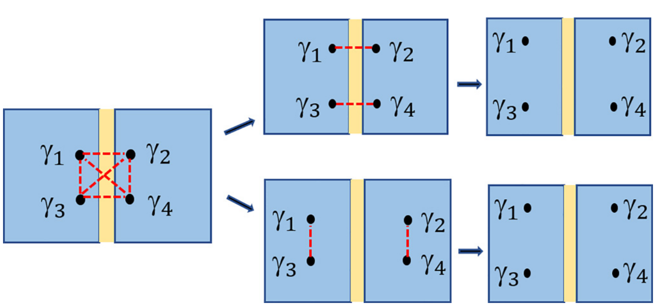

FIG. 3. The proposal for testing the non-Abelian fusion of MZMs. Initially, all four Majoranas are coupled with each other. The upper and lower paths correspond to different ways of adiabatically decoupling the Majoranas, leading to different final states.

path and the lower one, the corresponding final state would be $|0_{12}, 0_{34}\rangle$ and $|0_{13}, 0_{24}\rangle = \frac{1}{\sqrt{2}}(|0_{12}, 0_{34}\rangle - i|1_{12}, 1_{34}\rangle)$ respectively, and therefore they can be distinguished by the qubit-readout procedure we have discussed above: the upper path results in a 4π Josephson current as $\frac{4e}{\hbar}\Gamma\sin\frac{\phi}{2}$ with a probability of 100%, while the lower one leads to a current as $\frac{4e}{\hbar}\Gamma\sin\frac{\phi}{2}$ or $-\frac{4e}{\hbar}\Gamma\sin\frac{\phi}{2}$ with probability of 50%, respectively.

V. DISCUSSION AND SUMMARY

The above setup bases itself on preparing a topological superconducting system containing only four MZMs in experiments; therefore it may be realized in a superconducting island. However, we may also propose an alternative experimental scheme to implement our current measurement, in which a dual-probe scanning tunneling microscope (STM) setup is required. In this case, the restriction of a four-MZM system may be released. Two connected STM probes are in alignment with γ_1, γ_2 and two more the same with γ_3, γ_4 (four STM probes are needed in total), forming two independent circuits with the Josephson current as current resources, respectively, which can avoid not only the interference of MZMs in other vortices, but also the difficulty of growing normal metal leads at both ends of the Josephson junction in experiments. Furthermore, due to the relation $\phi = 2\pi\Phi/\Phi_0$, where the magnetic flux quantum $\Phi_0 = hc/2e$, and the fact that the magnetic field B applied in the ring in Fig. 1 should be weak enough to have less influence on the existence of MZMs compared with the one that can host MZMs, which is about 0.5 T [14], hence by assuming $B \leqslant 0.5$ T and $\phi = 4\pi$ at least owing to the period of the fractional Josephson current, we can easily come to the conclusion that the magnitude of the ring's area should at least be around 10^{-1} μm^2.

In general, taking advantage of the fact that MZMs can be hosted in vortices in intrinsic topological iron-based superconductors as discussed before, we propose a feasible scheme to read out the qubit information encoded in the MZMs through projective measurements on a Josephson junction, instead of measuring the precise 4π Josephson current, which in reality is commonly affected by unknown factors, this setup allows us to reveal the system's state through the reverse of the MZM-induced component of Josephson current that arises from the non-Abelian statistics of Majorana fermions, leading to the verification of the existence of MZMs. The results derived above are from the non-Abelian statistics of the MZMs so that the arrived at conclusions may not be changed by some possible nontopological subgap states.

Moreover, we identify the relationship of the transmission coefficient D and the size of the Josephson junction W_y and W_z to ensure we can distinguish the current difference between two measurements. We further show that an arbitrary Majorana vortex qubit can be read out after a series of projective measurements based on our setup, offering an experimentally promising possibility of showing the existence and their braiding statistics of Majorana fermions.

ACKNOWLEDGMENTS

This work is supported by the Training Program of Major Research plan of the National Natural Science Foundation of China (Grant No. 92165105). This work is supported in part by the NSFC (Grants No. 11974348 and No. 11834014), and the National Key R&D Program of China (Grant No. 2018YFA0305800). It is also supported by the Fundamental Research Funds for the Central Universities, and the Strategic Priority Research Program of CAS (Grants No. XDB28000000 and No. XDB33000000).

APPENDIX A: THE SOLUTION OF THE BdG EQUATION OF SPINLESS $p_x + ip_y$ SUPERCONDUCTOR

The mean-field BCS Hamiltonian of the spinless $p_x + ip_y$ superconductor is defined as

$$H_{\rm BCS} = \int d^2\boldsymbol{r}\,\hat{\psi}^\dagger(\boldsymbol{r})\left(-\frac{\hbar^2\nabla^2}{2m} - \mu\right)\hat{\psi}(\boldsymbol{r}) + \frac{i\hbar}{p_{\rm F}}\int d^2\boldsymbol{r}\,\Delta(\boldsymbol{r})\frac{\partial\hat{\psi}^\dagger(\boldsymbol{r})}{\partial\bar{z}}\hat{\psi}^\dagger(\boldsymbol{r}) + \text{ H.c.}, \tag{A1}$$

where the superconducting gap $\Delta(\boldsymbol{p}) = \frac{\Delta_0}{p_{\rm F}}(p_x + ip_y)$, $z = x + iy$. $\bar{z}$ is the complex conjugate of z. The BdG equation can be written as

$$H_{\rm BdG} = \begin{pmatrix} -\frac{\hbar^2\nabla^2}{2m} - \mu & \frac{i\hbar}{p_{\rm F}}\left\{\Delta(\boldsymbol{r}), \frac{\partial}{\partial\bar{z}}\right\} \\ \frac{i\hbar}{p_{\rm F}}\left\{\Delta^*(\boldsymbol{r}), \frac{\partial}{\partial z}\right\} & \frac{\hbar^2\nabla^2}{2m} + \mu \end{pmatrix}. \tag{A2}$$

Hence, we have

$$H_{\rm BdG}\begin{pmatrix} u_n(\boldsymbol{r}) \\ v_n(\boldsymbol{r}) \end{pmatrix} = E_n\begin{pmatrix} u_n(\boldsymbol{r}) \\ v_n(\boldsymbol{r}) \end{pmatrix}. \tag{A3}$$

The Hamiltonian $H_{\rm BdG}$ is invariant under transformation: $\sigma_1 H_{\rm BdG}\sigma_1 = -H_{\rm BdG}^*$. This symmetry implies that if $\Psi = (u_n, v_n)^T$ is a solution of Eq. (A3) with eigenvalue E_n, then $\sigma_1\Psi^* = (v_n^*, u_n^*)^T$ must be a solution with the eigenvalue $-E_n$. Thus, for a zero-energy state, we have the constraint $u = v^*$. From Eq. (A3), we have

$$\left(-\frac{\hbar^2\nabla^2}{2m} - \mu\right)u_n(\boldsymbol{r}) + \frac{i\hbar}{p_{\rm F}}\left\{\Delta(\boldsymbol{r}), \frac{\partial}{\partial\bar{z}}\right\}v_n(\boldsymbol{r}) = u_n(\boldsymbol{r})E_n. \tag{A4}$$

By transforming the formula from the Cartesian coordinates to cylindrical coordinates, we can obtain

$$\begin{aligned} &-\frac{\hbar^2}{2m}\left(\frac{1}{r}\frac{du_n(r)}{dr} + \frac{d^2u_n(r)}{dr^2} + \frac{1}{r^2}\frac{d^2u_n(r)}{d\varphi^2}\right)e^{i(\varphi-\pi/4)} \\ &-(\hbar^2)\left(\frac{i}{mr^2}\frac{du_n(r)}{d\varphi} - \frac{u_n(r)}{2mr^2}\right)e^{i(\varphi-\pi/4)} - \mu u_n(r)e^{i(\varphi-\pi/4)} \\ &-\frac{\hbar}{2p_{\rm F}}f(r)e^{i(\varphi-\pi/4)}\left(\frac{dv_n(r)}{dr} + \frac{i}{r}\frac{dv_n(r)}{d\varphi} + \frac{1}{r}v_n(r)\right) \\ &-\hbar\frac{e^{i(\varphi-\pi/4)}}{2p_{\rm F}}\left(\frac{d}{dr} + \frac{i}{r}\frac{d}{d\varphi}\right)[f(r)v_n(r)] \\ &= u_n(r)e^{i(\varphi-\pi/4)}E_n. \end{aligned} \tag{A5}$$

where $u_n(\boldsymbol{r}) = u_n(r,\varphi) = u_n(r)e^{i(\varphi-\pi/4)}$, $v_n(\boldsymbol{r}) = v_n(r,\varphi) = v_n(r)e^{i(\varphi-\pi/4)}$. As for zero mode, $E_n = 0$, $u_n(r) = v_n^*(r)$, and considering that we are looking for a solution to this equation in terms of a spherically symmetric real function $u(r)$, we can simplify it into

$$-\frac{\hbar^2}{2m}u_n''-\left(\frac{\hbar^2}{2mr}+\frac{f(r)}{\hbar p_{\rm F}}\right)u_n' +\left(\frac{\hbar^2}{2mr^2}-\frac{f(r)}{2\hbar p_{\rm F}r}-\frac{1}{2\hbar p_{\rm F}}\frac{df(r)}{dr}\right)u_n=\mu u_n, \quad \text{(A6)}$$

where $u_n''=\frac{d^2u_n}{dr^2}$ and $u_n'=\frac{du_n}{dr}$. Using the transformation

$$u_n(r)=\chi(r)\exp\left(-\frac{1}{\hbar v_{\rm F}}\int_0^r dr' f(r')\right), \quad \text{(A7)}$$

and substituting it into Eq. (A6), we get

$$\chi''(r)+\frac{1}{r}\chi'(r)+\left(\frac{2m\mu}{\hbar^2}-\frac{mf^2(r)}{p_{\rm F}v_{\rm F}\hbar^2}-\frac{1}{r^2}\right)\chi(r)=0, \quad \text{(A8)}$$

where the symbol of prime means derivation with respect to r. Since the order parameter of the superconductor

$$\Delta(r)=f(r)e^{i\phi}, \quad \text{(A9)}$$

where

$$f(r)=\Delta_0\tanh\left(\frac{r}{\xi}\right), \quad \text{(A10)}$$

and $r\ll\xi$, here we assume that $\Delta_0\ll\epsilon_{\rm F}$, which is typical for weak-coupling superconductors, hence

$$\frac{2m\mu}{\hbar^2}-\frac{mf^2(r)}{p_{\rm F}v_{\rm F}\hbar^2}=\frac{2m\mu}{\hbar^2}-\frac{m}{p_{\rm F}v_{\rm F}\hbar^2}\Delta_0^2\tanh^2\left(\frac{r}{\xi}\right)\approx\frac{p_{\rm F}^2}{\hbar^2}. \quad \text{(A11)}$$

Therefore

$$\chi''(r)+\frac{1}{r}\chi'(r)+\left(\frac{p_{\rm F}^2}{\hbar^2}-\frac{1}{r^2}\right)\chi(r)=0, \quad \text{(A12)}$$

and using the transformation $\tilde{r}=k_{\rm F}r$, and $p_{\rm F}=\hbar k_{\rm F}$, we have

$$\chi''(\tilde{r})+\frac{1}{\tilde{r}}\chi'(\tilde{r})+\left(1-\frac{1}{\tilde{r}^2}\right)\chi(\tilde{r})=0. \quad \text{(A13)}$$

It is a Bessel equation, and its solution is

$$\chi(\tilde{r})=AJ_1(\tilde{r}), \quad \text{(A14)}$$

i.e.,

$$\chi(k_{\rm F}r)=AJ_1(k_{\rm F}r), \quad \text{(A15)}$$

then

$$u(r,\varphi)=AJ_1(k_{\rm F}r)\exp\left[i(\varphi-\pi/4)-\frac{1}{\hbar v_{\rm F}}\int_0^r dr' f(r')\right] =v^*(r,\varphi), \quad \text{(A16)}$$

so

$$\Psi(\boldsymbol{r})=\begin{pmatrix}u_n(\boldsymbol{r})\\ v_n(\boldsymbol{r})\end{pmatrix} =AJ_1(k_{\rm F}r)\exp\left[-\frac{1}{\hbar v_{\rm F}}\int_0^r dr' f(r')\right]\begin{pmatrix}e^{i(\varphi-\pi/4)}\\ -e^{i(\varphi-\pi/4)}\end{pmatrix} \quad \text{(A17)}$$

with the normalization constant A. Although A is not relevant to our calculation, its expression can be found in Ref. [38]. This result will be used to estimate the distance of two MZMs denoted by R, which can be used in the further calculation of the $I_{\rm MZM}$.

APPENDIX B: THE JOSEPHSON CURRENT

Considering a 1D SIS Josephson junction with a p-wave superconducting coupling, the Hamiltonian of the junction can be written as

$$\mathcal{H}=\begin{pmatrix}\mathcal{H}_{\rm I}(k_x) & \mathcal{H}_{\rm S}(k_x)\\ \mathcal{H}_{\rm S}^*(k_x) & -\mathcal{H}_{\rm I}(k_x)\end{pmatrix} =\begin{pmatrix}\frac{\hbar^2k_x^2}{2m}-\mu+U_0\delta(x) & \Delta_\beta\frac{k_x}{k_{\rm F}}\\ \Delta_\beta^*\frac{k_x}{k_{\rm F}} & -\frac{\hbar^2k_x^2}{2m}+\mu-U_0\delta(x)\end{pmatrix}. \quad \text{(B1)}$$

We search solutions of the form

$$\psi_\beta=e^{\beta\kappa x}[A_\beta(u_{\beta,+};v_{\beta,+})^Te^{ik_{\rm F}x}+B_\beta(u_{\beta,-};v_{\beta,-})^Te^{-ik_{\rm F}x}], \quad \text{(B2)}$$

where a factor $\beta=+1$ (-1) is introduced for the left (right) electrode. Next we calculate κ. For $U_0=0$, the Schrödinger equation of $\mathcal{H}$ can be written as

$$\begin{pmatrix}-\frac{\hbar^2\partial^2}{2m\partial x^2}-\mu & \Delta(x)\\ \Delta^*(x) & \frac{\hbar^2\partial^2}{2m\partial x^2}+\mu\end{pmatrix}\begin{pmatrix}u(x)\\ v(x)\end{pmatrix}=E\begin{pmatrix}u(x)\\ v(x)\end{pmatrix}. \quad \text{(B3)}$$

The form of the solution to Eq. (B3) is assumed as

$$u(x)\equiv f(x)\exp(ik_{\rm F}x), \qquad v(x)\equiv g(x)\exp(ik_{\rm F}x), \quad \text{(B4)}$$

substituting it into Eq. (B3):

$$-\frac{\hbar^2}{2m}\frac{\partial^2}{\partial r^2}[e^{ik_{\rm F}x}f(x)]-\mu e^{ik_{\rm F}x}f(x)+\Delta(x)e^{ik_{\rm F}x}g(x) =-\frac{\hbar^2}{2m}\left[ik_{\rm F}^2e^{ik_{\rm F}x}f(x)+2ik_{\rm F}e^{ik_{\rm F}x}f'(x)+e^{ik_{\rm F}x}f''(x)\right] -\mu e^{ik_{\rm F}x}f(x)+\Delta(x)e^{ik_{\rm F}x}g(x) =Ee^{ik_{\rm F}x}f(x). \quad \text{(B5)}$$

Supposing the second-order term can be ignored compared with the first-order one, then the results read

$$-i\hbar v_{\rm F}f'(x)+\Delta(x)g(x)=Ef(x). \quad \text{(B6)}$$

Next taking $v(\mathbf{r})$ into Eq. (B3), similarly we have

$$i\hbar v_{\rm F}g'(x)+\Delta^*(x)f(x)=Eg(x), \quad \text{(B7)}$$

and combining Eqs. (B6) and (B7), we can obtain a Schrödinger-like equation for $f(x)$:

$$-(\hbar v_{\rm F})^2\frac{\partial^2f}{\partial x^2}+|\Delta(x)|^2f=E^2f(x). \quad \text{(B8)}$$

Therefore the solution of Eq. (B8) has the form of

$$f(x)=e^{\phi(x)/\hbar}, \quad \text{(B9)}$$

and substituting it into Eq. (B8),

$$\hbar^2 v_F^2 \phi''(x) + [\phi'(x)]^2 = \Delta_0^2 - E^2. \tag{B10}$$

The approximation $|\Delta(r)|^2 \approx |\Delta_0|^2$ is taken here, and further we can assume that

$$\phi'(x) = A(x) + iB(x) \equiv \frac{d\phi(x)}{dx}, \tag{B11}$$

where the amplitude of $f(x)$ is $\exp[\int^x A(x')dx'/\hbar]$, and $\exp[\int^x B(x')dx'/\hbar]$ is the phase part. Bring these into Eq. (B8) and matching the real and imaginary parts separately it yields

$$\begin{aligned}&\hbar^2 v_F^2 A'(x) + A(x)^2 - B(x)^2 = \Delta_0^2 - E^2,\\ &\hbar^2 v_F^2 B'(x) + 2A(x)B(x) = 0.\end{aligned} \tag{B12}$$

Next we expand $A(x)$ and $B(x)$ to the power of $\hbar$:

$$\begin{aligned}A(x) &= \sum_{n=0}^{\infty} \hbar^n A_n(x),\\ B(x) &= \sum_{n=0}^{\infty} \hbar^n B_n(x),\end{aligned} \tag{B13}$$

and substituting into Eq. (B12) and matching the zero-order term coefficients of $\hbar$ yields

$$A_0(x)^2 - B_0(x)^2 = \frac{\Delta_0^2 - E^2}{v_F^2}, \quad A_0(x)B_0(x) = 0. \tag{B14}$$

If the phase change is much slower than the wave amplitude, i.e., $B_0(x) \ll A_0(x)$, then we can assume

$$A_0(x) = \pm\frac{\sqrt{\Delta_0^2 - E^2}}{v_F}, \quad B_0(x) = 0. \tag{B15}$$

This equation only holds when $\Delta_0 \geqslant E$, and the quantum tunneling effect will appear. Substituting it into Eq. (B12) and matching the first-order term coefficients of $\hbar$ reads

$$\begin{aligned}&A_0' + 2A_0A_1 - 2B_0B_1 = A_0' + 2A_0A_1 = 0,\\ &B_0' + 2A_0B_1 + 2A_1B_0 = 2A_0B_1 = 0,\end{aligned} \tag{B16}$$

and we can easily have

$$\begin{aligned}&B_1 = 0,\\ &A_1 = -\frac{A_0'}{2A_0} = \frac{d}{dx}\ln A_0^{-1/2}.\end{aligned} \tag{B17}$$

Hence, by now combining the results in Eqs. (B15) and (B17), the phase part is

$$\begin{aligned}&\exp\left[\int^x B(x')dx'/\hbar\right]\\ &= \exp\left[\int^x [B_0(x') + B_1(x')]dx'/\hbar\right] = 1,\end{aligned} \tag{B18}$$

and the amplitude reads

$$\begin{aligned}\exp\left[\int^x A(x')dx'/\hbar\right] &= \exp\left[\int [(A_0(x') + A_1(x')]dx'/\hbar\right]\\ &= \frac{1}{\sqrt{A_0}} e^{\pm(1/\hbar)\int A_0(x')dx'}\\ &= \frac{1}{\sqrt{p(x)}} e^{\pm(1/\hbar)\int p(x')dx'},\end{aligned} \tag{B19}$$

with $p(x) = \frac{\sqrt{\Delta_0^2 - E^2}}{v_F}$. Hence under WKB approximation with $\Delta_0 \geqslant E$, we can finally obtain

$$f(x) \propto e^{\pm\kappa x} = e^{\beta\left(\sqrt{\Delta_0^2 - E^2}/\hbar v_F\right)x}, \tag{B20}$$

where $1/\kappa$ represents the length scale over which the wave function decays away from the interface. Now taking Eq. (B2) into Eq. (B3), we can obtain

$$\begin{aligned}&\left(-\frac{\hbar^2\partial^2}{2m\partial^2 x} - \mu\right)(e^{\beta\kappa x}e^{ik_F x}u_{\beta,+}) - \Delta_{\beta,+}\frac{i\partial}{k_F\partial x}(e^{\beta\kappa x}e^{ik_F x}v_{\beta,+})\\ &= E e^{\beta\kappa x}e^{ik_F x}u_{\beta,+},\end{aligned} \tag{B21}$$

which can be simplified as

$$\begin{aligned}&\left[\frac{-\hbar^2(\beta\kappa + ik_F)^2}{2m} - \mu\right]u_{\beta,+} - \Delta_{\beta,+}\frac{i(\beta\kappa + ik_F)}{k_F}v_{\beta,+}\\ &= E u_{\beta,+},\end{aligned} \tag{B22}$$

in the limit of $k_F \gg \kappa$, we can obtain

$$\begin{aligned}\eta_{\beta,+} = \frac{v_{\beta,+}}{u_{\beta,+}} &= \frac{E + \frac{\hbar^2(\beta\kappa + ik_F)^2}{2m} + \mu}{-\Delta_{\beta,+}\frac{i(\beta\kappa + ik_F)}{k_F}}\\ &\approx \frac{E + \frac{i\hbar^2\beta\kappa k_F}{m} - \frac{\hbar^2 k_F^2}{2m} + \mu}{\Delta_{\beta,+}}\\ &= \frac{E + i\beta\kappa\hbar v_F}{\Delta_{\beta,+}}.\end{aligned} \tag{B23}$$

Similarly we have

$$\eta_{\beta,-} = \frac{v_{\beta,-}}{u_{\beta,-}} = \frac{E - i\beta\kappa\hbar v_F}{\Delta_{\beta,-}}, \tag{B24}$$

where

$$\begin{aligned}&\Delta_{L,+} = \Delta_0, \quad \Delta_{R,+} = \Delta_0 e^{i\phi},\\ &\Delta_{L,-} = \Delta_0, \quad \Delta_{R,-} = \Delta_0 e^{i\phi}.\end{aligned} \tag{B25}$$

The geometry of a junction constrains the solutions of Eq. (B1) with two boundary conditions at the interface ($x = 0$):

$$\begin{aligned}&\psi_L(x=0) = \psi_R(x=0),\\ &\frac{\partial\psi_L}{\partial x}(x=0) - \frac{\partial\psi_R}{\partial x}(x=0) = k_F Z_0 \psi_{L/R}(x=0),\end{aligned} \tag{B26}$$

with $Z_0 = \frac{2mU_0}{\hbar^2 k_F}$, thus we can obtain the 4×4 linear system of equations

$$\begin{aligned}A_L u_{L,+} + B_L u_{L,-} &= A_R u_{R,+} + B_R u_{R,-},\\ A_L v_{L,+} + B_L v_{L,-} &= A_R v_{R,+} + B_R v_{R,-},\\ Z_0(A_L u_{L,+} + B_L u_{L,-}) &= i(A_R u_{R,+} - B_R u_{R,-}\\ &\quad - A_L u_{L,+} + B_L u_{L,-}),\\ Z_0(A_L v_{L,+} + B_L v_{L,-}) &= i(A_R v_{R,+} - B_R v_{R,-}\\ &\quad - A_L v_{L,+} + B_L v_{L,-}).\end{aligned} \tag{B27}$$

This 4×4 linear system with $A_{\rm L}, B_{\rm L}, A_{\rm R}, B_{\rm R}$ only has nonzero solutions if its determinant is zero, i.e.,

$$\begin{vmatrix} u_{\rm L,+} & u_{\rm L,-} & -u_{\rm R,+} & -u_{\rm R,-} \\ v_{\rm L,+} & v_{\rm L,-} & -v_{\rm R,+} & -v_{\rm R,-} \\ (Z_0+i)u_{\rm L,+} & (Z_0-i)u_{\rm L,-} & -iu_{\rm R,+} & iu_{\rm R,-} \\ (Z_0+i)v_{\rm L,+} & (Z_0-i)v_{\rm L,-} & -iv_{\rm R,+} & iv_{\rm R,-} \end{vmatrix} = 0, \tag{B28}$$

which can be written as

$$\begin{aligned} &4u_{\rm R,+}u_{\rm R,-}v_{\rm L,+}v_{\rm L,-} - 4u_{\rm L,+}u_{\rm R,-}v_{\rm L,-}v_{\rm R,+} \\ &\quad - 4u_{\rm L,-}u_{\rm R,+}v_{\rm L,+}v_{\rm R,-} + 4u_{\rm L,+}u_{\rm L,-}v_{\rm R,+}v_{\rm R,-} \\ &\quad + u_{\rm L,-}u_{\rm R,-}v_{\rm L,+}v_{\rm R,+}Z_0^2 - u_{\rm L,+}u_{\rm R,-}v_{\rm L,-}v_{\rm R,+}Z_0^2 \\ &\quad - u_{\rm L,-}u_{\rm R,+}v_{\rm L,+}v_{\rm R,-}Z_0^2 + u_{\rm L,+}u_{\rm R,-}v_{\rm L,-}v_{\rm R,-}Z_0^2 = 0. \end{aligned} \tag{B29}$$

Then dividing the equation by $u_{\rm R,+}u_{\rm R,-}v_{\rm L,+}v_{\rm L,-}$, it reads

$$\begin{aligned} &4 - 4\frac{\eta_{\rm R,+}}{\eta_{\rm L,+}} - 4\frac{\eta_{\rm R,-}}{\eta_{\rm L,-}} + 4\frac{\eta_{\rm R,+}\eta_{\rm R,-}}{\eta_{\rm L,+}\eta_{\rm L,-}} + Z_0^2\frac{\eta_{\rm R,+}}{\eta_{\rm L,-}} - Z_0^2\frac{\eta_{\rm R,+}}{\eta_{\rm L,+}} \\ &- Z_0^2\frac{\eta_{\rm R,-}}{\eta_{\rm L,-}} + Z_0^2\frac{\eta_{\rm R,-}}{\eta_{\rm L,+}} = 0, \end{aligned} \tag{B30}$$

which can be simplified as

$$\begin{aligned} &4(\eta_{\rm R,+}-\eta_{\rm L,+})(\eta_{\rm R,-}-\eta_{\rm L,-}) \\ &\quad = Z_0^2(\eta_{\rm R,+}-\eta_{\rm R,-})(\eta_{\rm L,-}-\eta_{\rm L,+}). \end{aligned} \tag{B31}$$

Finally we have

$$\frac{(\eta_{\rm R,-}-\eta_{\rm L,-})(\eta_{\rm R,+}-\eta_{\rm L,+})}{(\eta_{\rm R,+}-\eta_{\rm L,-})(\eta_{\rm R,-}-\eta_{\rm L,+})} = 1-D, \tag{B32}$$

with the transmission coefficient

$$D = \frac{4}{4+Z_0^2}. \tag{B33}$$

Then substituting Eqs. (B23) and (B24) into Eq. (B32), we can obtain

$$\begin{aligned} &\frac{\left(\frac{E-i\kappa\hbar v_{\rm F}}{\Delta_0 e^{i\phi}} - \frac{E+i\kappa\hbar v_{\rm F}}{\Delta_0}\right)\left(\frac{E+i\kappa\hbar v_{\rm F}}{\Delta_0 e^{i\phi}} - \frac{E-i\kappa\hbar v_{\rm F}}{\Delta_0}\right)}{\left(\frac{E-i\kappa\hbar v_{\rm F}}{\Delta_0 e^{i\phi}} - \frac{E+i\kappa\hbar v_{\rm F}}{\Delta_0 e^{i\phi}}\right)\left(\frac{E-i\kappa\hbar v_{\rm F}}{\Delta_0} - \frac{E+i\kappa\hbar v_{\rm F}}{\Delta_0}\right)} \\ &= \frac{[(E-a)e^{-i\phi}-(E+a)][(E+a)e^{-i\phi}-(E-a)]}{[(E-a)e^{-i\phi}-(E+a)e^{-i\phi}][(E-a)-(E+a)]} \\ &= \frac{e^{-i\phi}+e^{i\phi}-2\frac{2E^2-\Delta_0^2}{\Delta_0^2}}{2\frac{2E^2-\Delta_0^2}{\Delta_0^2}-2} = \frac{1-D}{D}, \end{aligned} \tag{B34}$$

Finally the energy-phase relation in a 1D p-wave Josephson junction can be derived with the above equation as

$$E_{px} \equiv E = \pm\Delta_0\sqrt{D}\cos(\phi/2). \tag{B35}$$

Here we consider the ground state, i.e., $E_{px} = -\Delta_0\sqrt{D}\cos(\phi/2)$, hence

$$I_{px} = \frac{e\Delta_0}{\hbar}\sqrt{D}\sin(\phi/2). \tag{B36}$$

Similarly, as for the 1D s-wave Josephson junction,

$$\begin{aligned} E_{s_x}(\phi) &= -\Delta_0\sqrt{1-D\sin^2(\phi/2)}, \\ I_{s_x} &= \frac{e\Delta_0 D\sin\phi}{\hbar\sqrt{1-D\sin^2\frac{\phi}{2}}}. \end{aligned} \tag{B37}$$

[1] E. Majorana, Il Nuovo Cimento **14**, 171 (1937).
[2] L. Fu and C. L. Kane, Phys. Rev. Lett. **100**, 096407 (2008).
[3] J. D. Sau, R. M. Lutchyn, S. Tewari, and S. Das Sarma, Phys. Rev. Lett. **104**, 040502 (2010).
[4] R. M. Lutchyn, J. D. Sau, and S. Das Sarma, Phys. Rev. Lett. **105**, 077001 (2010).
[5] Y. Oreg, G. Refael, and F. von Oppen, Phys. Rev. Lett. **105**, 177002 (2010).
[6] R. X. Zhang, W. S. Cole, and S. Das Sarma, Phys. Rev. Lett. **122**, 187001 (2019).
[7] L. P. Rokhinson, X. Liu, and J. K. Furdyna, Nat. Phys. **8**, 795 (2012).
[8] M. T. Deng, C. L. Yu, G. Y. Huang, M. Larsson, P. Caroff, and H. Q. Xu, Nano Lett. **12**, 6414 (2012).
[9] A. Das, Y. Ronen, Y. Most, Y. Oreg, M. Heiblum, and H. Shtrikman, Nat. Phys. **8**, 887 (2012).
[10] H. O. H. Churchill, V. Fatemi, K. Grove-Rasmussen, M. T. Deng, P. Caroff, H. Q. Xu, and C. M. Marcus, Phys. Rev. B **87**, 241401(R) (2013).
[11] S. Nadj-Perge, I. K. Drozdov, J. Li, H. Chen, S. Jeon, J. Seo, A. H. MacDonald, B. A. Bernevig, and A. Yazdani, Science **346**, 602 (2014).
[12] S. M. Albrecht, A. P. Higginbotham, M. Madsen, F. Kuemmeth, T. S. Jespersen, J. Nygård, P. Krogstrup, and C. M. Marcus, Nature (London) **531**, 206 (2016).
[13] J. P. Xu, M. X. Wang, Z. L. Liu, J. F. Ge, X. Yang, C. Liu, Z. A. Xu, D. Guan, C. L. Gao, D. Qian, Y. Liu, Q. H. Wang, F. C. Zhang, Q. K. Xue, and J. F. Jia, Phys. Rev. Lett. **114**, 017001 (2015).
[14] D. Wang, L. Kong, P. Fan, H. Chen, S. Zhu, W. Liu, L. Cao, Y. Sun, S. Du, J. Schneeloch, R. Zhong, G. Gu, L. Fu, H. Ding, and H. J. Gao, Science **362**, 333 (2018).
[15] T. Machida, Y. Sun, S. Pyon, S. Takeda, Y. Kohsaka, T. Hanaguri, T. Sasagawa, and T. Tamegai, Nat. Mater. **18**, 811 (2019).
[16] Q. Liu, C. Chen, T. Zhang, R. Peng, Y. J. Yan, Chen-Hao-Ping Wen, X. Lou, Y. L. Huang, J. P. Tian, X. L. Dong, G. W. Wang, W. C. Bao, Q. H. Wang, Z. P. Yin, Z. X. Zhao, and D. L. Feng, Phys. Rev. X **8**, 041056 (2018).
[17] M. J. Gray, J. Freudenstein, S. Y. F. Zhao, R. O'Connor, S. Jenkins, N. Kumar, M. Hoek, A. Kopec, S. Huh, T. Taniguchi, K. Watanabe, R. Zhong, C. Kim, G. D. Gu, and K. S. Burch, Nano Lett. **19**, 4890 (2019).
[18] Z. Wang, J. O. Rodriguez, L. Jiao, S. Howard, M. Graham, G. D. Gu, T. L. Hughes, D. K. Morr, and V. Madhavan, Science **367**, 104 (2020).
[19] N. Read and D. Green, Phys. Rev. B **61**, 10267 (2000).
[20] C. Beenakker, Annu. Rev. Condens. Matter Phys. **4**, 113 (2013).
[21] S. D. Sarma, M. Freedman, and C. Nayak, npj Quantum Inf. **1**, 15001 (2015).

[22] C. Nayak, S. H. Simon, A. Stern, M. Freedman, and S. Das Sarma, Rev. Mod. Phys. **80**, 1083 (2008).
[23] K. T. Law, P. A. Lee, and T. K. Ng, Phys. Rev. Lett. **103**, 237001 (2009).
[24] K. Sengupta, I. Žutić, H. J. Kwon, V. M. Yakovenko, and S. Das Sarma, Phys. Rev. B **63**, 144531 (2001).
[25] J. D. Sau, S. Tewari, R. Lutchyn, T. Stanescu, and S. Das Sarma, Phys. Rev. B **82**, 214509 (2010).
[26] G. Koren, T. Kirzhner, E. Lahoud, K. B. Chashka, and A. Kanigel, Phys. Rev. B **84**, 224521 (2011).
[27] V. Mourik, K. Zuo, S. M. Frolov, S. R. Plissard, E. P. A. M. Bakkers, and L. P. Kouwenhoven, Science **336**, 1003 (2012).
[28] P. Zhang, K. Yaji, T. Hashimoto, Y. Ota, T. Kondo, K. Okazaki, Z. Wang, J. Wen, G. D. Gu, H. Ding, and S. Shin, Science **360**, 182 (2018).
[29] G. Xu, B. Lian, P. Tang, X. L. Qi, and S. C. Zhang, Phys. Rev. Lett. **117**, 047001 (2016).
[30] E. J. H. Lee, X. Jiang, R. Aguado, G. Katsaros, C. M. Lieber, and S. De Franceschi, Phys. Rev. Lett. **109**, 186802 (2012).
[31] S. Hikami, A. I. Larkin, and Y. Nagaoka, Prog. Theor. Phys. **63**, 707 (1980).
[32] N.-H. Kim, Y.-S. Shin, H.-S. Kim, J.-D. Song, and Y.-J. Doh, Curr. Appl. Phys. **18**, 384 (2018).
[33] I. S. Veshchunov, W. Magrini, S. V. Mironov, A. G. Godin, J.-B. Trebbia, A. I. Buzdin, P. Tamarat, and B. Lounis, Nat. Commun. **7**, 12801 (2016).
[34] E. W. J. Straver, J. E. Hoffman, O. M. Auslaender, D. Rugar, and K. A. Moler, Appl. Phys. Lett. **93**, 172514 (2008).
[35] O. M. Auslaender, L. Luan, E. W. J. Straver, J. E. Hoffman, N. C. Koshnick, E. Zeldov, D. A. Bonn, R. Liang, W. N. Hardy, and K. A. Moler, Nat. Phys. **5**, 35 (2008).
[36] A. Kremen, S. Wissberg, N. Haham, E. Persky, Y. Frenkel, and B. Kalisky, Nano Lett. **16**, 1626 (2016).
[37] A. Y. Kitaev, Phys. Usp. **44**, 131 (2001).
[38] M. Cheng, R. M. Lutchyn, V. Galitski, and S. Das Sarma, Phys. Rev. Lett. **103**, 107001 (2009).
[39] H. Miao, P. Richard, Y. Tanaka, K. Nakayama, T. Qian, K. Umezawa, T. Sato, Y. M. Xu, Y. B. Shi, N. Xu, X. P. Wang, P. Zhang, H. B. Yang, Z. J. Xu, J. S. Wen, G. D. Gu, X. Dai, J. P. Hu, T. Takahashi, and H. Ding, Phys. Rev. B **85**, 094506 (2012).
[40] L. Y. Kong and H. Ding, Acta. Phys. Sin. **69**, 110301 (2020).
[41] Y. Asano, Y. Tanaka, M. Sigrist, and S. Kashiwaya, Phys. Rev. B **67**, 184505 (2003).
[42] J. Alicea, Y. Oreg, G. Refael, F. von Oppen, and M. P. A. Fisher, Nat. Phys. **7**, 412 (2011).
[43] L. Embon, Y. Anahory, A. Suhov, D. Halbertal, J. Cuppens, A. Yakovenko, A. Uri, Y. Myasoedov, M. L. Rappaport, M. E. Huber, A. Gurevich, and E. Zeldov, Sci. Rep. **5**, 7598 (2015).
[44] C. K. Chiu, T. Machida, Y. Huang, T. Hanaguri, and F. C. Zhang, Sci. Adv. **6**, eaay0443 (2020).
[45] C. X. Liu, D. E. Liu, F. C. Zhang, and C. K. Chiu, Phys. Rev. Appl. **12**, 054035 (2019).